Applied Catalysis B: Environmental 308 (2022) 121217

Contents lists available at ScienceDirect

Applied Catalysis B: Environmental

journal homepage: www.elsevier.com/locate/apcatb

SO_2-enhanced nitrate photolysis on TiO_2 minerals: A vital role of photochemically reactive holes

Huan Shang [a], Ziyue Chen [a], Xiao Wang [b], Meiqi Li [a], Hao Li [a], Chengliang Mao [a], Linghao Yu [a], Jing Sun [b], Zhihui Ai [a,*], Lizhi Zhang [a,*]

[a] Key Laboratory of Pesticide & Chemical Biology of Ministry of Education, Institute of Environmental & Applied Chemistry, College of Chemistry, Central China Normal University, Wuhan 430079, PR China
[b] Shanghai Institute of Ceramics, Chinese Academy of Sciences, Shanghai 200050, PR China

ARTICLE INFO

Keywords:
Nitrate photolysis
Heterogeneous SO_2 oxidation
TiO_2 mineral
Photochemistry
HONO

ABSTRACT

In this study, we investigated the nitrate photolysis on photoactive TiO_2 particles in the presence of SO_2 through theoretic DFT calculation and in situ DRIFTS analysis, and found that in a clean atmosphere nitrate was oxidized to $\bullet NO_3$ radicals by the holes generated on the surface of TiO_2 under solar irradiation, followed reactive nitrogen species generation via $\bullet NO_3$ radicals reduction by photoinduced electrons. After shifting to the SO_2-polluted environment, $\bullet NO_3$ radicals preferentially reacted with abundant sulfites to significantly increase nitrogen species formation, the online measured concentrations of NO_x and HONO increased by approximately 2-fold and 6-fold respectively in comparison with clean atmosphere. These results demonstrate that photogenerated holes play a key role in nitrate photolysis on photoactive mineral dusts with or without the coexistence of SO_2, providing new insights into the source of NO_x and HONO in complex air polluted areas during the daytime.

1. Introduction

In regions polluted by nitrogen oxides (NO_x = NO, NO_2), nitrate is ubiquitously deposited over the atmospheric particles due to the oxidation of NO_x [1–4]. Atmospheric nitrate is known to be a crucial contribution to the formation of secondary inorganic aerosol, photochemical smog and haze, causing severe air pollution problems [5–8]. Recently, many groups reported that nitrate was not the ultimate oxidation product of NO_x in the atmosphere [9–13]. Once deposited on the reactive surfaces such as snow, leaves, metal and mineral dust, nitrate can be photochemically decomposed to reactive nitrogen species (NO_x, HONO) [12–17]. This surface-enhanced nitrate photolysis can lead to a rapid release of NO_x and HONO into the atmosphere and subsequently affect the atmospheric oxidative capacity [17–19].

Mineral dusts are the predominant components of ambient particle matters in the urban atmosphere [20,21]. Particularly, the mineral surfaces provide sufficient reactive sites for atmospheric NO_x oxidation, resulting in nitrate deposition on the mineral dusts [20,21]. Therefore, systematic investigating the interaction between nitrate and mineral dusts is of great significance for understanding the photolysis of nitrate in the atmosphere. Regarding the extensive use of semiconductor coating materials, mineral dusts become more and more photochemically active, which might significantly affect nitrate photolysis processes [22–24]. For example, Ndour et al. reported that TiO_2 could activate the photolysis of nitrate into NO_x, because the photogenerated holes react with nitrate to form a nitrate radical and then trigger nitrate photolysis [25]. However, the influence of the photogenerated electrons on the nitrate photolysis is yet unclear.

Field observations revealed a strong correlation between nitrate (NO_x) and sulfate (or SO_2) on mineral particles [26,27], and recent studies also highlighted the significant interaction of nitrate with SO_2 on mineral oxides [28–33]. For instance, Zhang et al. demonstrated that nitrate could enhance the heterogeneous oxidation of SO_2 on authentic mineral dusts by the accumulation of protons, during which HONO was released as the product of nitrate reduction [33]. Ma et al. reported the promotive effect of SO_2 on the photolysis of NH_4NO_3 on TiO_2 for the yields of NO_2 and HONO due to the acidity and site competition of sulfate generated by SO_2 oxidation [34]. However, in these literature reports, the nitrate decomposition mechanism on photoactive minerals with the coexistence of SO_2 still remains unknown at the molecular level.

Given that TiO_2 is a typical photoactive mineral dust [35–38], this

* Corresponding authors.
E-mail addresses: jennifer.ai@mail.ccnu.edu.cn (Z. Ai), zhanglz@mail.ccnu.edu.cn (L. Zhang).

https://doi.org/10.1016/j.apcatb.2022.121217
Received 6 December 2021; Received in revised form 29 January 2022; Accepted 12 February 2022
Available online 15 February 2022

study systematically investigated the heterogeneous photolysis mechanism of nitrate on TiO_2 particles in the presence of SO_2 using the first-principles density of functional theory (DFT) calculations and in situ diffuse reflectance Fourier transformed infrared spectroscopy (in situ DRIFTS). Our results revealed that photogenerated holes capable of activating nitrate to $\bullet NO_3$ radicals play an important role in the SO_2-enhanced nitrate photolysis on photoactive mineral dusts, strongly contributing to the formation of NO_x and HONO in complex air polluted areas during the daytime.

2. Experimental section

2.1. Sample preparation

All chemicals employed in this study are of analytical grade and used without any further purification. Pristine TiO_2 particles were commercial TiO_2 (Degussa P25). Nitrate-loaded TiO_2 particles containing 10 wt % of $NaNO_3$ were prepared via an impregnation method [17]. In a typical procedure, 0.15 g TiO_2 particles were immersed into 10 mL $NaNO_3$ solution (1.5 mg/mL), and the resulting suspension was vigorously stirred for 20 min and dried at 70 °C without filtration. The prepared nitrate-absorbed TiO_2 sample was denoted as NO_3^-/TiO_2. For comparison, nitrate-attached alumina (NO_3^-/Al_2O_3) was prepared in the same procedure.

2.2. Gases products measurement

Nitrate photolysis on TiO_2 particles was performed in a continuous flow reactor with volume of 4.5 L at ambient temperature (298 K) (Fig. S1). In a typical procedure, 0.15 g of prepared sample was added into 10 mL of H_2O and dispersed evenly by ultrasonic washer, and then the resulting suspension was placed on a glass dish with a diameter of 10 cm. The coated dish was dried at 70 °C for water evaporation to obtain a catalyst film. The prepared film was placed in the reactor using Xenon lamp (PLS-MW2000, Beijing Perfect Light Co., Ltd., China) as solar light. A compressed SO_2 (100 ppm, Ar balance) was diluted to about 1 ppm by the air stream supplied by an air generator. When adsorption-desorption equilibrium was achieved, the lamp was turned on. Gases products (NO_x and HONO) were continuously detected by NO_x analyzer (Teledyne, MODEL T200), in which molybdenum converters could convert HONO and NO_2 to NO and carbonate denuder is capable of trapping HONO [39]. The HONO concentration was indirectly verified as the difference in the NO_2 signals with and without carbonate denuder. To avoid the saturation effect, a new Na_2CO_3 denuder was installed before each absorption experiment.

3. Results and discussion

3.1. Theoretical calculation analysis

As typical surface of TiO_2 minerals, the anatase TiO_2 (101) exposing with fully coordinated atoms (Ti_{6c} and O_{3c}) and undercoordinated atoms (Ti_{5c} and O_{2c}) is used in this study. DFT calculations are employed to investigate the adsorption of O_2, nitrate and SO_2 on the surface of TiO_2 minerals under combined atmospheric pollution. As shown in Fig. 1, the adsorption energy of nitrate (2.94 eV) via Ti site on the TiO_2 surface is higher than that of O_2 (1.05 eV) and SO_2 (0.80 eV) (Fig. 1a-c), indicating that nitrate is preferentially adsorbed on the TiO_2 surface. O_2 also tends

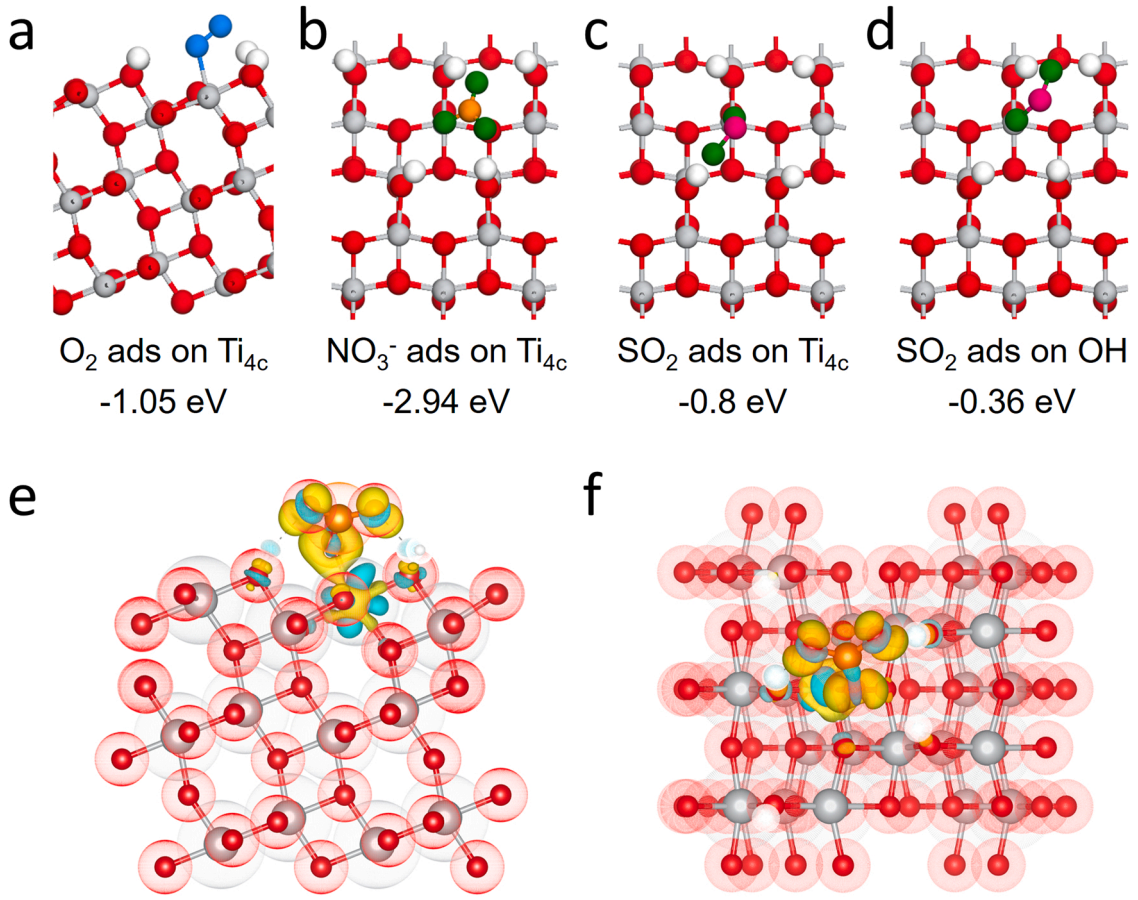

Fig. 1. Adsorption configurations of reaction molecules on TiO_2: (a) O_2, (b) nitrate, (c) SO_2 via Ti site, (d) SO_2 via OH site. The charge density difference calculations of nitrate-adsorbed TiO_2: (e) front view and (f) top view. The isovalue is 0.015 au. The yellow and blue isosurfaces represent charge accumulation and depletion in the space, respectively. (For interpretation of the references to colour in this figure legend, the reader is referred to the web version of this article.)

to bind to the Ti site with the moderate oxygen affinity, competing with the nitrate adsorbed on the surface. In contrast, SO_2 preferentially bonds with surface -OH due to its weak adsorption energy (0.36 eV, Fig. 1d). Generally, SO_2 could adsorb on undercoordinated O_{2c} (H) site or surface hydroxyl sites via H bonds to convert into sulfites on the surface of TiO_2. The photocatalytic oxidation of SO_2 on the surface of TiO_2 takes place via an Eley-Rideal mechanism [40–44]. Surface Ti or vacancy on the TiO_2 activates the adsorbed O_2 to $\bullet O_2^-$, which can directly convert SO_2 into sulfate [43,44]. Obviously, oxygen adsorption and molecular oxygen activation are vital for SO_2 oxidation. Based on the DFT calculations, nitrate can preoccupy the reactive Ti sites on TiO_2 in the coexistence of SO_2, which could hinder the oxidation of SO_2. However, it has been reported that the reduction of nitrate can be accelerated by sulfite formed by SO_2 adsorption, while sulfite can be transformed into sulfates [33,34]. Thus, we hypothesized that there is a synergistic interaction between nitrate and SO_2 on the surface of semiconductor minerals (for example TiO_2) during the SO_2 polluted atmosphere.

Further charge density difference calculations clearly show that covalent-bonding nitrate gains extra electrons as soon as adsorbed on the surface Ti site under the solar irradiation (Fig. 1e and f), leading to improvement of nitrate photolysis. After nitrate photolysis, the occupied Ti sites on TiO_2 surface are released, thus facilitating reactive oxygen species (ROS) generation by molecular oxygen activation and simultaneous formation of sulfite. This mutually-reinforced interaction between nitrate and SO_2 on minerals could be one of the critical factors for the secondary inorganic aerosol formation in SO_2-polluted regions.

3.2. *Characterization of the nitrate-adsorbed TiO_2 particles*

Inspired by DFT theoretical calculation results, nitrate-adsorbed TiO_2 (NO_3^-/TiO_2) was prepared using a facile impregnation method (Fig. 2). The compositions of the prepared particles were determined by XRD patterns (Fig. 2a). A series of diffraction peaks of NO_3^-/TiO_2 coincided well with those in the standard card of anatase TiO_2 (JCPDS No. 1–562) and rutile TiO_2 (JCPDS No. 1–1292), indicating that TiO_2 maintained original crystal structures after nitrate impregnation. A prominent diffraction peak at 29.4° was attributed to the (104) diffraction plane of $NaNO_3$ (JCPDS No. 1–840), suggesting the uniform nitrate dispersion on the surface of TiO_2. The chemical composition of nitrate-adsorbed TiO_2 was further confirmed by Raman and XPS analysis. Raman analysis of NO_3^-/TiO_2 exhibited a characteristic peak of nitrate at 1070 cm^{-1} (Fig. 2b). The corresponding XPS spectra also detected the presence of nitrate on the surface of TiO_2 (Fig. 2c-e). This was revealed by two obvious peaks of O 1 *s* and N 1 *s* at 533.0 and 407.2 eV, respectively, which were ascribed to the O-N of nitrate [45,46]. And the valence states of Ti and O in NO_3^-/TiO_2 particles remained as those of pristine TiO_2, suggesting that the introduction of nitrate did not affect the electron density of TiO_2. As revealed by the HRTEM

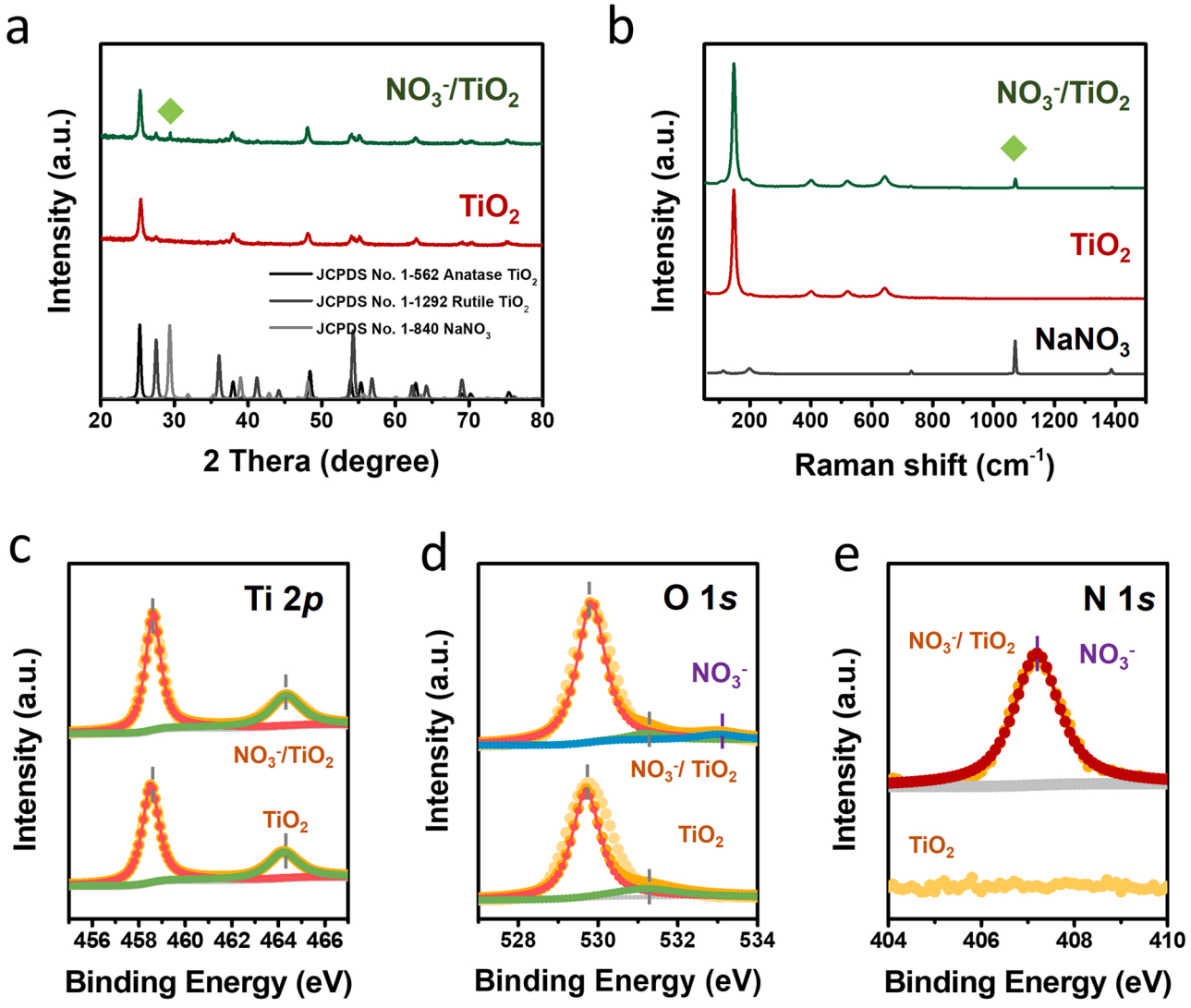

Fig. 2. (a) The XRD patterns; (b) Raman spectra; (c) Ti *2p* XPS analysis; (d) O *1 s* XPS analysis; (e) N *1 s* XPS analysis.

images (Fig. S2), the NO_3^-/TiO_2 particles were of granular morphology with a lattice spacing of 0.35 nm corresponding to the (101) surface of TiO_2. The BET surface areas of pristine TiO_2 and NO_3^-/TiO_2 are 35 and 44 m^2/g respectively (Fig. S3), 25% of BET increase implied that NO_3^- deposition could provide more active sites for nitrate renoxification and SO_2 oxidation on TiO_2 in complex atmospheric pollution.

3.3. SO_2 enhanced nitrate photolysis on TiO_2 particles

Nitrate photolysis on TiO_2 samples was measured by a continuous stream reactor experiments. In the absence of TiO_2 samples, the concentrations of NO and NO_2 on the $NaNO_3$ salt particles increased slightly under the solar irradiation with or without the coexistence of SO_2 (Fig. S4a). The weak nitrate photolysis without additional interface implied that nitrate photolysis was surface-dependent heterogeneous reaction, and required minerals particles to provide (photo-)active sites. In order to verify this deduction, light inactive Al_2O_3 was introduced as the reaction interface. It was observed that Al_2O_3 containing with $NaNO_3$ (NO_3^-/Al_2O_3) remained inactive under solar irradation, since little reactive nitrogen species were observed (Fig. S4b). In contrast, NO_3^-/TiO_2 constantly released reactive nitrogen species upon exposure to solar irradiation, approximately 35 ppb of NO, 24 ppb of NO_2 and 22 ppb of HONO were online measured (Fig. 3a and b). This implied that nitrate photolysis was controlled only by photoactive sites of minerals upon light-induced heterogeneous processing of nitrate and TiO_2. After introducing SO_2, approximately 100 ppb of NO, 64 ppb of NO_2 and 153 ppb of HONO were online detected during nitrate photolysis on TiO_2, which was increased by approximately 2-fold NO_x and 6-fold HONO respectively in comparison with clean atmosphere (Fig. 3a and b). KNO_3 was added as a control, and the photolysis of nitrate promoted by SO_2 was also observed on the surface of KNO_3/TiO_2 under solar irradiation (Fig. S5). Based on above measurements, we believe that the photogenerated electrons and holes on TiO_2 play important roles in the photochemical renoxification of nitrate (Fig. 3c), SO_2 abundantly coexist in the atmosphere could significantly contribute to nitrate photolysis by changing reaction pathway over TiO_2. We continued to investigate the reaction of SO_2 and NO on the mineral surface and found that NO_x will not be accumulated on the TiO_2 mineral surface, and SO_2 mainly reacts with nitrate to release active nitrogen species on the TiO_2 mineral under solar irradiation (Fig. S6).

3.4. Proposed nitrate photolysis mechanism

Due to the photochemical activity of TiO_2, the photogenerated carriers tend to generate reactive oxygen species via the molecular oxygen activation, which may affect the photolysis of nitrate and the photooxidation of SO_2. Thus, the photogenerated carriers and reactive oxygen species should be carefully analyzed. First, the role of O_2 in nitrate photolysis was investigated with or without SO_2. We found that nitrate photolysis on TiO_2 was significantly enhanced in the absence of O_2 (Fig. S7). The main product of nitrate reduction was NO (314 ppb), which was much higher than that in the presence of O_2 (35 ppb). And the yield of NO_2 and HONO (~ 20 ppb) decreased correspondingly, suggesting that they may be mainly formed by secondary oxidation of NO. Rapid release of NO was also observed on TiO_2 in the presence of SO_2 (Fig. S7). These results indicated that O_2 was not conducive to nitrate photolysis on TiO_2, with or without SO_2 coexistence [34,47]. There is a reasonable prospect that nitrate would preferentially convert to NO through the three-electron pathway ($NO_3^- \rightarrow NO$), since there is no O_2 competing to electrons [17]. In addition, sulfites formed by SO_2 adsorption avoid being oxidized to sulfates by O_2, thus, nitrate photolysis could be further enhanced by the reaction between sulfites and nitrates (Fig. S7). By contrast, the release of active nitrogen species on TiO_2 without SO_2 coexistence was much higher than that in the coexistence of SO_2. This might be because sulfites were less reductive than electrons [33], and the promoting effect of SO_2 was weakened in the absence of O_2 (Fig. S7).

Subsequently, trapping experiments were used to further reveal the heterogeneous reaction mechanism on NO_3^-/TiO_2 surface (Figs. 4 and S8). As revealed by the results, both electrons and holes play the critical roles in nitrate photolysis on TiO_2 surface (Figs. 4a and S8). The yield of NO increased after $\bullet O_2^-$ trapping, while the yields of NO_2 and HONO

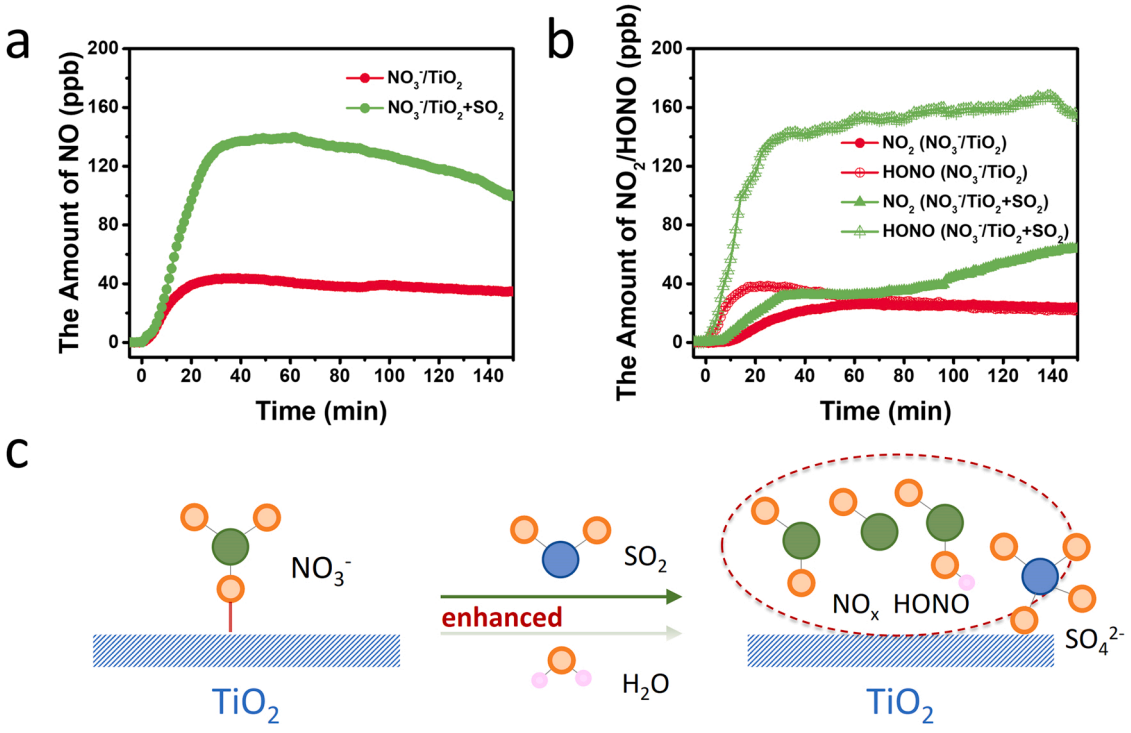

Fig. 3. Online measured concentrations of (a) NO, (b) NO_2 and HONO during the photochemical reaction of NO_3^-/TiO_2 in the presence of SO_2; (c) Schematic diagram of nitrate photolysis on the surface of TiO_2 in the presence of SO_2.

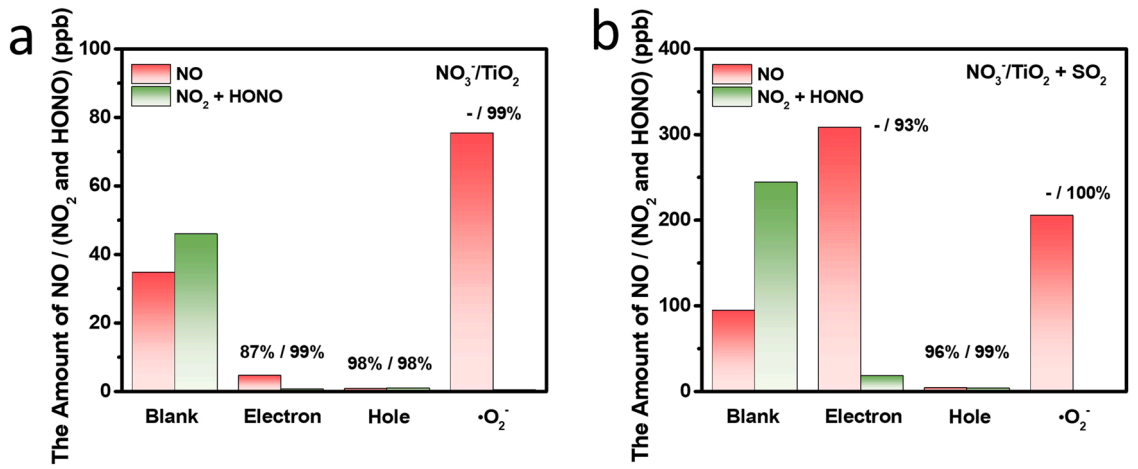

Fig. 4. Influence of different scavengers on the photolysis of nitrate on NO_3^-/TiO_2 in clean environment (a) and in the presence of SO_2 (b).

were inhibited. This indicated that NO_2 and HONO were mainly derived from the secondary oxidation of NO. Interestingly, the active species of nitrate photolysis were holes in the presence of SO_2 (Figs. 4b and S8). When the reduction of electrons was inhibited, the observed yield of NO increased dramatically, but the yields of NO_2 and HONO decreased by 93%. It is known that nitrate photolysis on mineral generally occurs via the electron reduction and reducing agent reaction, such as sulfite, which is formed by the adsorption of SO_2 [33]. This implied that the

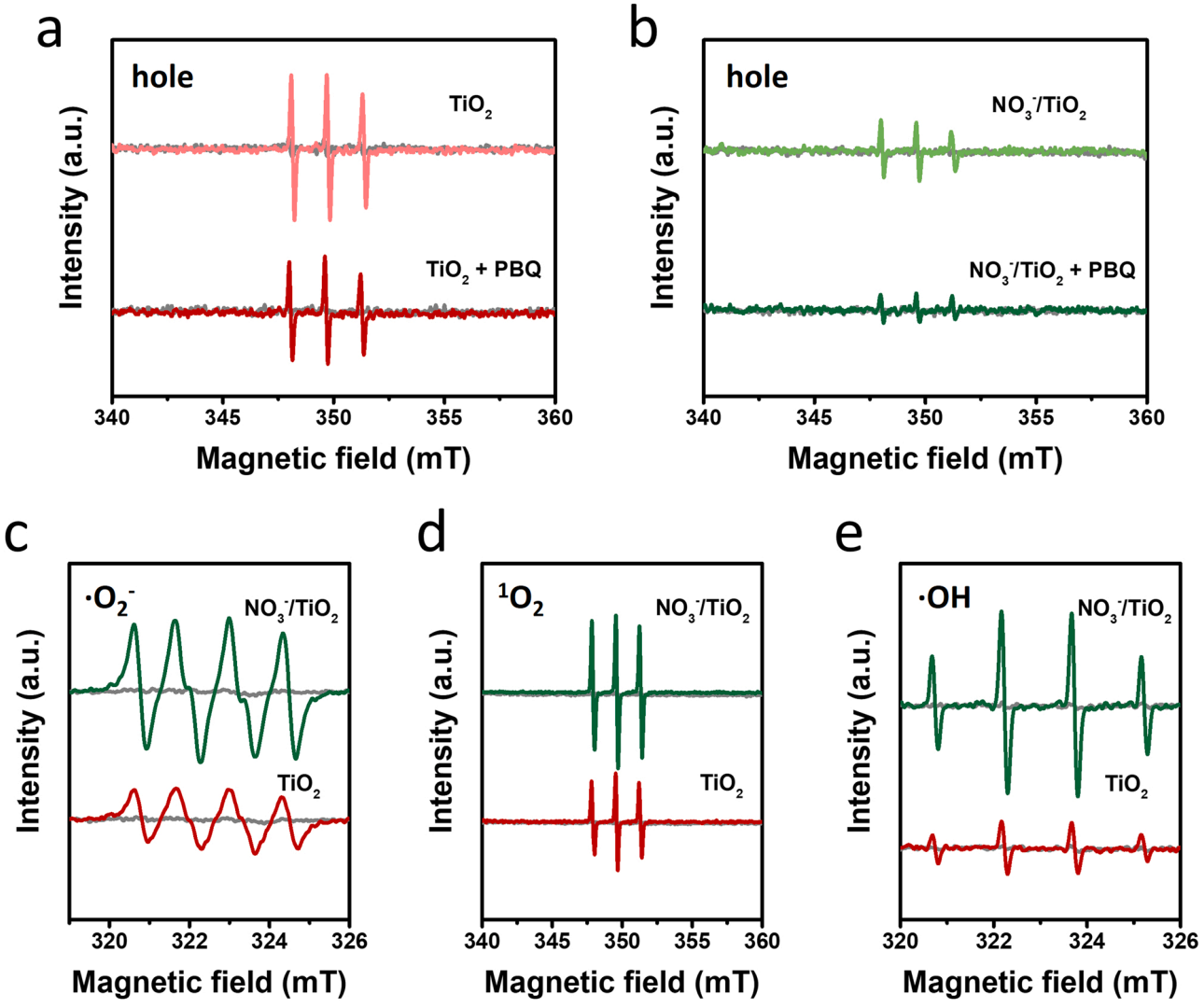

Fig. 5. ESR spectra of the spin-reactive holes generated by (a) TiO_2 and (b) NO_3^-/TiO_2; ESR spectra of (c) $\bullet O_2^-$, (d) $^1O_2$, (e) •OH generated by TiO_2 and NO_3^-/TiO_2 under solar irradiation.

three-electron reduction product of nitrate (NO) could be produced through the redox reaction between nitrate and surface sulfite. Besides, $\bullet O_2^-$ capture leaded to the surge of NO and total inhibition of NO_2 and HONO, suggesting that NO_2 and HONO could also be formed by partial oxidation of sulfite in addition to the secondary oxidation of NO, as evidenced by the experimental results in the absence of O_2 (Fig. S7). In conclusion, the existence of SO_2 can change the photolysis pathway of nitrate on TiO_2 and greatly promote the release of reactive nitrogen species, implying that the combined gas pollution will have a more severe impact on the atmospheric environment.

ESR spin trapping was further applied to identify the reactive species formed in NO_3^-/TiO_2 particles (Fig. 5). First, 1-hydroxy-3-carboxy-2,2,5,5-tetramethylpyrrolidine (CPH) was chosen to verify the generation of holes induced by TiO_2 and NO_3^-/TiO_2 particles, as it can be oxidized by holes to form CP• radicals with a typical three-line ESR signal [48]. Given that $\bullet O_2^-$ could also induce CP• ESR signals by oxidation reaction, p-benzoquinone (PBQ) was employed as a trapping reagent of $\bullet O_2^-$. As expected, the addition of PBQ significantly reduced the CP• ESR signals both for TiO_2 and NO_3^-/TiO_2 particles. Importantly, the holes signal intensity of TiO_2 (maximum intensity, 0.25 a.u.) was still higher than that (maximum intensity, 0.08 a.u.) of NO_3^-/TiO_2 (Fig. 5a and b). Based on the results of trapping experiments, we believe that the partial (~70%) reduction in hole signals can be attributed to the presence of nitrate. That is to say, the highly reactive holes may react with nitrates to generate nitrate radicals [49,50], which depleted the holes and thus triggered the decomposition of nitrate. For comparison of each ROS produced by TiO_2 and NO_3^-/TiO_2 particles, we observed an increase in the ESR signals of $\bullet O_2^-$, $^1O_2$ and •OH on NO_3^-/TiO_2 particles (Fig. 5c-e). This increase was attributable to the reaction between holes and nitrates, inhibiting the recombination of electrons. More electrons were therefore used to activate molecular oxygen to generate the ROS, this further facilitated the oxidation of SO_2.

To experimentally investigate the possible mechanism of nitrate photolysis on TiO_2 particles in the presence of SO_2, a series of techniques were performed (Fig. 6). As the TPD experiments showed, the desorption peaks of O_2 on TiO_2 and NO_3^-/TiO_2 were 480 and 663 ℃, respectively (Fig. 6a). This indicated that NO_3^-/TiO_2 was more conducive for adsorption and activation of O_2 in comparison with TiO_2. The desorption peaks of SO_2 on the TiO_2 surface were 245, 440 and 667 ℃ respectively, corresponding to SO_2 adsorbed at the surface hydroxyl, Ti site and lattice oxygen site (Fig. 6b) [44]. Similarly, the adsorption of SO_2 on NO_3^-/TiO_2 surface could also be attributed to the above adsorption states. Compared with pristine TiO_2, there was no obvious shift of the characteristic peaks of SO_2 on NO_3^-/TiO_2 surface, suggesting that nitrate deposition did not affect the adsorption mode of SO_2 on TiO_2. Moreover, the peak intensity of SO_2 on NO_3^-/TiO_2 was slightly weakened, suggesting the competitive adsorption of nitrate on Ti site, which was consistent with the theoretical calculation results (Fig. 1). Therefore, we believe that SO_2 is preferentially adsorbed at the OH sites for oxidation. After nitrate photolysis release sites, SO_2 can harvest more reaction sites of the NO_3^-/TiO_2 mineral for SO_2 oxidation.

In situ FTIR analysis of nitrate photolysis on NO_3^-/TiO_2 was carried out in the air with or without SO_2. In the air atmosphere, the characteristic peaks of nitrite (1540 cm^{-1}) and the adsorbed NO_2 (1722 cm^{-1}) appeared on the surface of NO_3^-/TiO_2 after illumination (Fig. 6c). As the reaction progressed, these peaks continued to increase, indicating that nitrate photolysis on NO_3^-/TiO_2 produced NO_2 and NO_2^- (Fig. 6d). Simultaneously, the characteristic peaks of adsorbed water and surface hydroxyl group (1592 and 3691 cm^{-1}) also increased, suggesting that both adsorbed water and surface hydroxyl group were involved in the photolysis of nitrate. Unfortunately, the characteristic peak of NO was not detected, probably because NO was easily desorbed into the gas phase environment. Combined with the capture experiments (Fig. 4 and S8), we believe that nitrate photolysis produced nitrogen compounds (NO, NO_2 and HONO) in the air atmosphere. At the TiO_2 mineral interface, NO could be reoxidized to form NO_2 and NO_2^-. The NO_2^- product further reacted with adsorbed water and surface hydroxyl groups to form HONO. When SO_2 was introduced into the reaction chamber, characteristic peaks of sulfate (1158 cm^{-1}), nitrite (1530 cm^{-1}) and adsorbed NO_2 (1722 cm^{-1}) appeared on the surface of NO_3^-/TiO_2 after illumination (Fig. 6e). This result indicated that nitrate photolysis and SO_2 photochemical oxidation occurred simultaneously on NO_3^-/TiO_2 particle. Moreover, the characteristic peaks of adsorbed water and surface hydroxyl group also increased with the reaction (Fig. 6f),

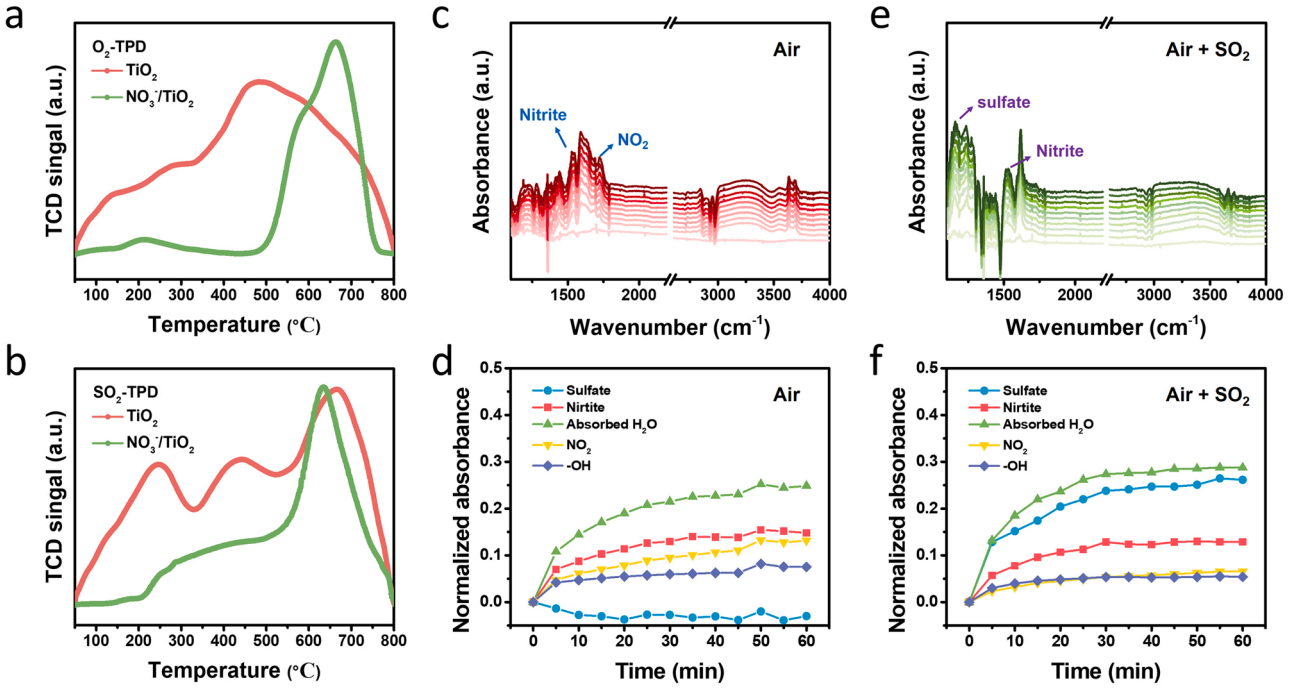

Fig. 6. (a) O_2-TPD analyses; (b) SO_2-TPD analyses; (c) FTIR spectra of nitrate photolysis on TiO_2 under air condition and (d) the corresponding absorbance of products; (e) FTIR spectra of nitrate photolysis on TiO_2 under air and SO_2 condition and (f) the corresponding absorbance of products.

confirming that water and hydroxyl group would participate in the surface reaction of TiO_2.

Subsequently, the in situ FTIR of nitrate photolysis proceeded on NO_3^-/TiO_2 particle under Ar condition was performed (Fig. S9). Compared with products intensity in air, the intensity of adsorbed NO_2 was significantly weakened in Ar atmosphere, as well as adsorbed water and hydroxyl (Fig. S9a and c), because nitrate photolysis mainly produced NO via the three-electron pathway due to the lack of molecular oxygen activation. Moreover, NO was not oxidized by O_2, avoiding the secondary oxidation of NO to NO_2 and NO_2^-. More importantly, in the mixed atmosphere of Ar and SO_2, the intensity of nitrite (NO_2) and sulfate on NO_3^-/TiO_2 surface was much higher than that under air condition (Fig. S9b and d). This result confirmed that the redox reaction between nitrate and sulfite occurred on the surface of TiO_2, where SO_2 was oxidized to sulfate and nitrate was reduced to reactive nitrogen species. We conducted XPS on the NO_3^-/TiO_2 samples after reaction (Fig. S10), and found that characteristic peaks of sulfites (168.3 eV) and sulfates (168.6 eV) appeared on the mineral surface with the coexistence of SO_2 after light irradiation. And the characteristic peak of nitrate (407.1 eV) was weakened after photolysis. This result also verified the interaction between sulfites and nitrate free radicals.

Based on theoretical DFT calculations and in situ FTIR experiments, nitrate photolysis on TiO_2 were summarized (Eqs. 1–16) (Fig. 7). In a clean atmosphere (in the absence of SO_2), the nitrate decomposition on TiO_2 surface was initiated by solar excitation (Fig. 7a). Under the solar irradiation, the excited TiO_2 produced photogenerated electrons and photogenerated holes (Eq. 1). And then photogenerated electrons reduced O_2 to produce ROS (Eq. 2), the photogenerated holes oxidized the adsorbed nitrates to form nitrate free radicals (Eq. 3) [50]. Nitrate free radicals could convert to NO and NO_2 through electron reduction through pathway a1 (Eq. 5) [50,51]. And ROS species further oxidized NO to form NO_2 and HONO (with water) (Eqs. 4, 6–9). Therefore, nitrate photolysis on TiO_2 semiconductors play a vatal role in the nitrogen cycle, implying that secondary aerosol pollution could be greatly accelerated by nitrate photolysis on semiconductor particles, especially in industrial areas with high semiconductor pollution.

$$TiO_2 + light \rightarrow electron + hole \quad (1)$$

$$Ti_{5c}\text{-}O_2 + electron \rightarrow Ti_{5c}\text{-}\bullet O_2^- \quad (2)$$

$$NO_3^- + hole \rightarrow \bullet NO_3 \quad (3)$$

$$H_2O + hole \rightarrow H^+ + \bullet OH \quad (4)$$

$$\bullet NO_3 + electron \rightarrow NO / NO_2 \text{ (pathway a1)} \quad (5)$$

$$NO + \bullet OH \rightarrow NO_2^- + H^+ \quad (6)$$

$$NO_2^- + H_2O \rightarrow HONO + OH^- \quad (7)$$

$$NO_2^- + H^+ \rightarrow NO + \bullet OH \quad (8)$$

$$NO + ROS \rightarrow NO_2 / HONO / NO_3^- \quad (9)$$

In the SO_2-polluted atmospheric environment, nitrate photolysis could be further enhanced by reductive sulfites on the surface of TiO_2 minerals (Eqs. 10–18) in addition to the above self-renoxification (Fig. 7b). Under the solar irradiation, nitrate was first oxidized to nitrate radical by holes (Eq. 3). At the initial stage of reaction, nitrate radicals preferentially reacted with abundant sulfites to form multi-electron reduction product (NO) through pathway b1 (Eq. 12) [30, 32]. NO_2 and HONO were mainly formed by the reoxidation of NO (Eqs. 6–9). With the consumption of surface sulfites and the accumulation of surface hydroxyl groups, NO could be further converted into NO_2^- by excess -OH through pathway b2 (Eq. 13). The intermediate NO_2^- reacted with H^+ (H_2O) to produce NO (HONO). Meanwhile, SO_2 can also be oxidized to sulfate by reactive oxygen species (Eqs. 10, 11, 14–18). Therefore, SO_2-enhanced photolysis of nitrate on the TiO_2 semiconductor surface should be responsible for the substantial release of NO_x and HONO in the atmosphere, the redox reaction between nitrate and surface sulfur-containing species would significantly affect the atmospheric photochemical processes of nitrate and sulfate on the surface of semiconductor minerals.

$$SO_{2\ (g)} + Ti\text{-}O^{2-}{}_{(lattice)} \rightarrow Ti\text{-}SO_3^{2-}{}_{(ads)} \quad (10)$$

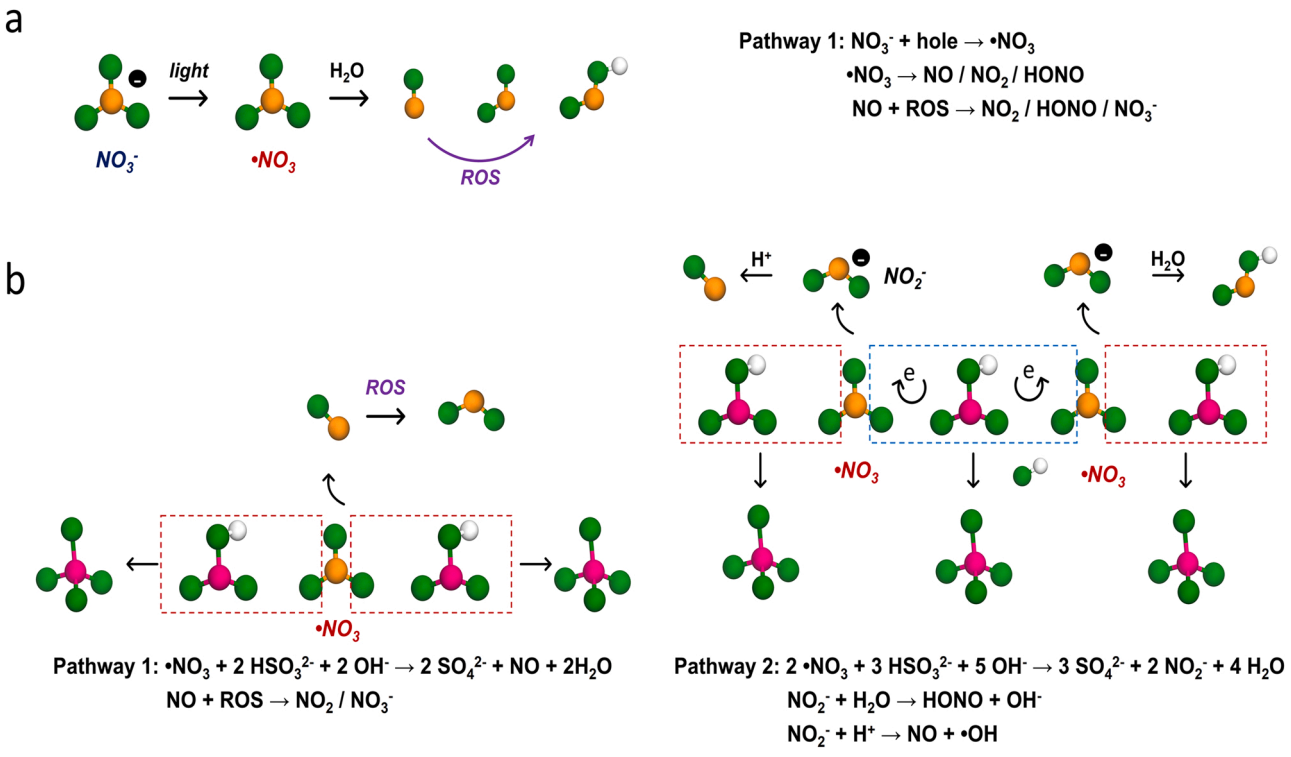

Fig. 7. Suggested mechanism for nitrate photolysis on TiO_2 (a) in the absence of SO_2 and (b) in the presence of SO_2.

$$SO_{2\ (g)} + \text{Ti-OH} \rightarrow \text{Ti-}HSO_{3\ (ads)} \quad (11)$$

$$\bullet NO_3 + 2\ HSO_3^{2-} + 2\ OH^- \rightarrow 2\ SO_4^{2-} + NO + 2\ H_2O \text{ (pathway b1)} \quad (12)$$

$$2\ \bullet NO_3 + 3\ HSO_3^{2-} + 5\ OH^- \rightarrow 3\ SO_4^{2-} + 2\ NO_2^- + 4\ H_2O \text{ (pathway b2)} \quad (13)$$

$$SO_2 + Ti_{5c}\text{-}\bullet O_2^- + \text{electron} \rightarrow SO_4^{2-} \quad (14)$$

$$\text{Ti-}SO_3^{2-} + \bullet O_2^- + \text{electron} \rightarrow \text{Ti-}O^{2-} + SO_4^{2-} \quad (15)$$

$$SO_2 + 2\ \bullet OH \rightarrow H_2SO_4 \quad (16)$$

$$SO_2 + H_2O \rightarrow 2\ H^+ + SO_3^{2-}{}_{(aq)} \quad (17)$$

$$SO_3^{2-}{}_{(aq)} + \bullet O_2^- \rightarrow SO_4^{2-}{}_{(aq)} + O^- \quad (18)$$

4. Conclusions

This study demonstrates that atmospheric photoactive semiconductor minerals are important factors affecting the photolysis of nitrate and oxidation of SO_2. TiO_2 minerals have the potential to initiate the nitrate activation to $\bullet NO_3$ radicals and therefore substantially release reactive nitrogen species via electron-reduction. When nitrate-containing TiO_2 minerals transported into the industrial or urban regions with server SO_2 pollutions, nitrate photolysis will be amplified by the redox reaction between nitrate and surface sulfites on TiO_2 minerals. These findings can well explain the positive correlation (0.92) between HONO and sulfate observed in the haze episodes [52]. Our work illustrates the promotive effect of SO_2 in nitrate photolysis on photoactive mineral dusts at the molecular level and helps to better understand the source of NO_x and HONO in complex air pollution areas during the daytime. Inspired by this study, the photochemistry of semiconductor minerals containing nitrate is worthy of more attention in SO_2-polluted regions, such as the North China Plain with high concentrations of mineral dust [3,29]. And coordinated control of NO_x, SO_2 and particulate pollution needs further study.

CRediT authorship contribution statement

Zhihui Ai, Lizhi Zhang and Huan Shang designed the study. **Zhihui Ai, Lizhi Zhang and Jing Sun** provided the supports on experimental feasibility. **Huan Shang, Xiao Wang, Hao Li, Meiqi Li, Chengliang Mao, Pan Xing, Shengxi Zhao and Ziyue Chen** performed characterizations and analyses under the supervision of **Zhihui Ai and Lizhi Zhang. Huan Shang, Meiqi Li, Hao Li and Chengliang Mao** performed the VASP calculations. **Huan Shang** wrote the paper. **Zhihui Ai, Lizhi Zhang** revised the paper. All authors contributed to the interpretation of the results and improvement of the paper.

Declaration of Competing Interest

The authors declare that they have no known competing financial interests or personal relationships that could have appeared to influence the work reported in this paper.

Acknowledgements

This work was supported by the National Key Research and Development Program of China (grant number 2016YFA0203000); National Science Foundation of China (grant numbers U20A20129, 21876058); and the 111 Project B17019.

Appendix A. Supporting information

Supplementary data associated with this article can be found in the online version at doi:10.1016/j.apcatb.2022.121217.

References

[1] F.J. Dentener, G.R. Carmichael, Y. Zhang, J. Lelieveld, P.J. Crutzen, Role of mineral aerosol as a reactive surface in the global troposphere, J. Geophys. Res. Atmos. 101 (1996) 22869–22889.
[2] C.R. Usher, A.E. Michel, V.H. Grassian, Reactions on mineral dust, Chem. Rev. 103 (2003) 4883–4940.
[3] X.Y. Zhang, Y.Q. Wang, T. Niu, X.C. Zhang, S.L. Gong, Y.M. Zhang, J.Y. Sun, Atmospheric aerosol compositions in China: spatial/temporal variability, chemical signature, regional haze distribution and comparisons with global aerosols, Atmos. Chem. Phys. 12 (2012) 779–799.
[4] J. Gao, S. Wang, Z. Li, L. Wang, Z. Chen, J. Zhou, High nitrate accumulation in the vadose zone after land-use change from croplands to orchards, Environ. Sci. Technol. 55 (2021) 5782–5790.
[5] A.E. Orel, J.H. Seinfeld, Nitrate formation in atmospheric aerosols, Environ. Sci. Technol. 11 (1977) 1000–1007.
[6] J. Finlayson-Pitts Barbara, N. Pitts James, Tropospheric air pollution: ozone, airborne toxics, polycyclic aromatic hydrocarbons, and particles, Science 276 (1997) 1045–1051.
[7] R. Atkinson, Atmospheric chemistry of VOCs and NO_x, Atmos. Environ. 34 (2000) 2063–2101.
[8] K. Lu, H. Fuchs, A. Hofzumahaus, Z. Tan, H. Wang, L. Zhang, S.H. Schmitt, F. Rohrer, B. Bohn, S. Broch, H. Dong, G.I. Gkatzelis, T. Hohaus, F. Holland, X. Li, Y. Liu, Y. Liu, X. Ma, A. Novelli, P. Schlag, M. Shao, Y. Wu, Z. Wu, L. Zeng, M. Hu, A. Kiendler-Scharr, A. Wahner, Y. Zhang, Fast photochemistry in wintertime haze: consequences for pollution mitigation strategies, Environ. Sci. Technol. 53 (2019) 10676–10684.
[9] J. Schuttlefield, G. Rubasinghege, M. El-Maazawi, J. Bone, V.H. Grassian, Photochemistry of adsorbed nitrate, J. Am. Chem. Soc. 130 (2008) 12210–12211.
[10] A.M. Baergen, D.J. Donaldson, Photochemical renoxification of nitric acid on real urban grime, Environ. Sci. Technol. 47 (2013) 815–820.
[11] L. Liu, X. Zhang, Y. Zhang, W. Xu, X. Liu, X. Zhang, J. Feng, X. Chen, Y. Zhang, X. Lu, S. Wang, W. Zhang, L. Zhao, Dry particulate nitrate deposition in China, Environ. Sci. Technol. 51 (2017) 5572–5581.
[12] C. Ye, H. Gao, N. Zhang, X. Zhou, Photolysis of nitric acid and nitrate on natural and artificial surfaces, Environ. Sci. Technol. 50 (2016) 3530–3536.
[13] C. Ye, N. Zhang, H. Gao, X. Zhou, Photolysis of particulate nitrate as a source of HONO and NO_x, Environ. Sci. Technol. 51 (2017) 6849–6856.
[14] X. Zhou, N. Zhang, M. TerAvest, D. Tang, J. Hou, S. Bertman, M. Alaghmand, P. B. Shepson, M.A. Carroll, S. Griffith, S. Dusanter, P.S. Stevens, Nitric acid photolysis on forest canopy surface as a source for tropospheric nitrous acid, Nat. Geosci. 4 (2011) 440–443.
[15] H.W. Jacobi, J. Kleffmann, G. Villena, P. Wiesen, M. King, J. France, C. Anastasio, R. Staebler, Role of nitrite in the photochemical formation of radicals in the snow, Environ. Sci. Technol. 48 (2014) 165–172.
[16] J. Liu, H. Deng, P.S.J. Lakey, H. Jiang, M. Mekic, X. Wang, M. Shiraiwa, S. Gligorovski, Unexpectedly high indoor HONO concentrations associated with photochemical NO_2 transformation on glass windows, Environ. Sci. Technol. 54 (2020) 15680–15688.
[17] F. Bao, M. Li, Y. Zhang, C. Chen, J. Zhao, Photochemical aging of Beijing urban $PM_{2.5}$: HONO production, Environ. Sci. Technol. 52 (2018) 6309–6316.
[18] Z. Liu, Y. Wang, F. Costabile, A. Amoroso, C. Zhao, L.G. Huey, R. Stickel, J. Liao, T. Zhu, Evidence of aerosols as a media for rapid daytime HONO production over China, Environ. Sci. Technol. 48 (2014) 14386–14391.
[19] W. Zhang, S. Tong, C. Jia, L. Wang, B. Liu, G. Tang, D. Ji, B. Hu, Z. Liu, W. Li, Z. Wang, Y. Liu, Y. Wang, M. Ge, Different HONO sources for three layers at the urban area of Beijing, Environ. Sci. Technol. 54 (2020) 12870–12880.
[20] G. Rubasinghege, S. Elzey, J. Baltrusaitis, P.M. Jayaweera, V.H. Grassian, Reactions on atmospheric dust particles: surface photochemistry and size-dependent nanoscale Redox chemistry, J. Phys. Chem. Lett. 1 (2010) 1729–1737.
[21] C. George, M. Ammann, B. D'Anna, D.J. Donaldson, S.A. Nizkorodov, Heterogeneous photochemistry in the atmosphere, Chem. Rev. 115 (2015) 4218–4258.
[22] H. Chen, C.E. Nanayakkara, V.H. Grassian, Titanium dioxide photocatalysis in atmospheric chemistry, Chem. Rev. 112 (2012) 5919–5948.
[23] M.A. Kebede, M.E. Varner, N.K. Scharko, R.B. Gerber, J.D. Raff, Photooxidation of ammonia on TiO_2 as a source of NO and NO_2 under atmospheric conditions, J. Am. Chem. Soc. 135 (2013) 8606–8615.
[24] S. Philip, R.V. Martin, A. Van Donkelaar, J.W. Lo, Y. Wang, D. Chen, L. Zhang, P. S. Kasibhatla, S. Wang, Q. Zhang, Z. Lu, D.G. Streets, S. Bittman, D.J. Macdonald, Global chemical composition of ambient fine particulate matter for exposure assessment, Environ. Sci. Technol. 48 (2014) 13060–13068.
[25] M. Ndour, P. Conchon, B. D'Anna, O. Ka, C. George, Photochemistry of mineral dust surface as a potential atmospheric renoxification process, Geophys. Res. Lett. 36 (2009), L05816.
[26] L. Kong, Y. Yang, S. Zhang, X. Zhao, H. Du, H. Fu, S. Zhang, T. Cheng, X. Yang, J. Chen, D. Wu, J. Shen, S. Hong, L. Jiao, Observations of linear dependence between sulfate and nitrate in atmospheric particles, J. Geophys. Res. Atmos. 119 (2014) 341–361.
[27] Z. Cao, X. Zhou, Y. Ma, L. Wang, R. Wu, B. Chen, W. Wang, The concentrations, formations, relationships and modeling of sulfate, nitrate and ammonium (SNA) aerosols over China, Aerosol Air Qual. Res. 17 (2017) 84–97.
[28] S. Ge, G. Wang, S. Zhang, D. Li, Y. Xie, C. Wu, Q. Yuan, J. Chen, H. Zhang, Abundant NH_3 in China enhances atmospheric HONO production by promoting the heterogeneous reaction of SO_2 with NO_2, Environ. Sci. Technol. 53 (2019) 14339–14347.

[29] H. He, Y. Wang, Q. Ma, J. Ma, B. Chu, D. Ji, G. Tang, C. Liu, H. Zhang, J. Hao, Mineral dust and NOx promote the conversion of SO_2 to sulfate in heavy pollution days, Sci. Rep. 4 (2014) 4172.
[30] Q. Ma, T. Wang, C. Liu, H. He, Z. Wang, W. Wang, Y. Liang, SO_2 initiates the efficient conversion of NO_2 to HONO on MgO surface, Environ. Sci. Technol. 51 (2017) 3767–3775.
[31] F. Bao, H. Jiang, Y. Zhang, M. Li, C. Ye, W. Wang, M. Ge, C. Chen, J. Zhao, The key role of sulfate in the photochemical renoxification on real $PM_{2.5}$, Environ. Sci. Technol. 54 (2020) 3121–3128.
[32] C. Liu, H. Wang, Q. Ma, J. Ma, Z. Wang, L. Liang, W. Xu, G. Zhang, X. Zhang, T. Wang, H. He, Efficient conversion of NO to NO_2 on SO_2-Aged MgO under atmospheric conditions, Environ. Sci. Technol. 54 (2020) 11848–11856.
[33] Y. Zhang, F. Bao, M. Li, C. Chen, J. Zhao, Nitrate-enhanced oxidation of SO_2 on mineral dust: a vital role of a proton, Environ. Sci. Technol. 53 (2019) 10139–10145.
[34] Q. Ma, C. Zhong, J. Ma, C. Ye, Y. Zhao, Y. Liu, P. Zhang, T. Chen, C. Liu, B. Chu, H. He, Comprehensive Study about the photolysis of nitrates on mineral oxides, Environ. Sci. Technol. 55 (2021) 8604–8612.
[35] R.J. Gustafsson, A. Orlov, P.T. Griffiths, R.A. Cox, R.M. Lambert, Reduction of NO_2 to nitrous acid on illuminated titanium dioxide aerosol surfaces: implications for photocatalysis and atmospheric chemistry, Chem. Commun. (2006) 3936–3938.
[36] A. El Zein, Y. Bedjanian, Reactive uptake of HONO to TiO_2 surface: "dark" reaction, J. Phys. Chem. A 116 (2012) 3665–3672.
[37] C.J. Ostaszewski, N.M. Stuart, D.M.B. Lesko, D. Kim, M.J. Lueckheide, J.G. Navea, Effects of coadsorbed water on the heterogeneous photochemistry of nitrates adsorbed on TiO_2, J. Phys. Chem. A 122 (2018) 6360–6371.
[38] H. Niu, K. Li, B. Chu, W. Su, J. Li, Heterogeneous reactions between toluene and NO_2 on mineral particles under simulated atmospheric conditions, Environ. Sci. Technol. 51 (2017) 9596–9604.
[39] C. Han, W. Yang, Q. Wu, H. Yang, X. Xue, Heterogeneous photochemical conversion of NO_2 to HONO on the humic acid surface under simulated sunlight, Environ. Sci. Technol. 50 (2016) 5017–5023.
[40] T. Liu, A.W.H. Chan, J.P.D. Abbatt, Multiphase oxidation of sulfur dioxide in aerosol particles: implications for sulfate formation in polluted environments, Environ. Sci. Technol. 55 (2021) 4227–4242.
[41] J. Park, M. Jang, Z. Yu, Heterogeneous photo-oxidation of SO_2 in the presence of two different mineral dust particles: gobi and Arizona dust, Environ. Sci. Technol. 51 (2017) 9605–9613.
[42] Y. Zhang, F. Bao, M. Li, H. Xia, D. Huang, C. Chen, J. Zhao, Photoinduced uptake and oxidation of SO_2 on Beijing urban $PM_{2.5}$, Environ. Sci. Technol. 54 (2020) 14868–14876.
[43] Q. Ma, L. Wang, B. Chu, J. Ma, H. He, Contrary role of H_2O and O_2 in the kinetics of heterogeneous photochemical reactions of SO_2 on TiO_2, J. Phys. Chem. A 123 (2019) 1311–1318.
[44] H. Shang, X. Wang, H. Li, M. Li, C. Mao, P. Xing, S. Zhao, Z. Chen, J. Sun, Z. Ai, L. Zhang, Oxygen vacancies promote sulfur species accumulation on TiO_2 mineral particles, Appl. Catal. B: Environ. 290 (2021), 120024.
[45] O. Rosseler, M. Sleiman, V.N. Montesinos, A. Shavorskiy, V. Keller, N. Keller, M. I. Litter, H. Bluhm, M. Salmeron, H. Destaillats, Chemistry of NOx on TiO_2 surfaces studied by ambient pressure XPS: products, effect of UV irradiation, water, and coadsorbed K^+, J. Phys. Chem. Lett. 4 (2013) 536–541.
[46] C.E. Nanayakkara, P.M. Jayaweera, G. Rubasinghege, J. Baltrusaitis, V.H. Grassian, Surface photochemistry of adsorbed nitrate: the role of adsorbed water in the formation of reduced nitrogen species on α-Fe_2O_3 particle surfaces, J. Phys. Chem. A 118 (2014) 158–166.
[47] M.E. Monge, B. D'Anna, C. George, Nitrogen dioxide removal and nitrous acid formation on titanium oxide surfaces—an air quality remediation process? Phys. Chem. Chem. Phys. 12 (2010) 8991–8998.
[48] W. He, H.-K. Kim, W.G. Wamer, D. Melka, J.H. Callahan, J.-J. Yin, Photogenerated charge carriers and reactive oxygen species in ZnO/Au hybrid nanostructures with enhanced photocatalytic and antibacterial activity, J. Am. Chem. Soc. 136 (2014) 750–757.
[49] S.A. Styler, D.J. Donaldson, Photooxidation of atmospheric alcohols on laboratory proxies for mineral dust, Environ. Sci. Technol. 45 (2011) 10004–10012.
[50] N.K. Scharko, A.E. Berke, J.D. Raff, Release of nitrous acid and nitrogen dioxide from nitrate photolysis in acidic aqueous solutions, Environ. Sci. Technol. 48 (2014) 11991–12001.
[51] Q. Shi, Y. Tao, J.E. Krechmer, C.L. Heald, J.G. Murphy, J.H. Kroll, Q. Ye, Laboratory investigation of renoxification from the photolysis of inorganic particulate nitrate, Environ. Sci. Technol. 55 (2021) 854–861.
[52] N.A. Saliba, S.G. Moussa, G. El, Tayyar, Contribution of airborne dust particles to HONO sources, Atmos. Chem. Phys. Discuss. 14 (2014) 4827–4839.